

University of Wollongong

## Research Online

---

Faculty of Engineering and Information  
Sciences - Papers: Part B

Faculty of Engineering and Information  
Sciences

---

2019

# Development and evaluation of a comfort-oriented control strategy for thermal management of mixed-mode ventilated buildings

Massimo Fiorentini

*University of Wollongong, [massimo@uow.edu.au](mailto:massimo@uow.edu.au)*

Gianluca Serale

*Politecnico di Torino, [gianluca.serale@polito.it](mailto:gianluca.serale@polito.it)*

Georgios Kokogiannakis

*University of Wollongong, [gkg@uow.edu.au](mailto:gkg@uow.edu.au)*

Alfonso Capozzoli

*Politecnico di Torino, [alfonso.capozzoli@polito.it](mailto:alfonso.capozzoli@polito.it)*

Paul Cooper

*University of Wollongong, [pcooper@uow.edu.au](mailto:pcooper@uow.edu.au)*

Follow this and additional works at: <https://ro.uow.edu.au/eispapers1>



Part of the [Engineering Commons](#), and the [Science and Technology Studies Commons](#)

---

### Recommended Citation

Fiorentini, Massimo; Serale, Gianluca; Kokogiannakis, Georgios; Capozzoli, Alfonso; and Cooper, Paul, "Development and evaluation of a comfort-oriented control strategy for thermal management of mixed-mode ventilated buildings" (2019). *Faculty of Engineering and Information Sciences - Papers: Part B*. 3118.

<https://ro.uow.edu.au/eispapers1/3118>

Research Online is the open access institutional repository for the University of Wollongong. For further information contact the UOW Library: [research-pubs@uow.edu.au](mailto:research-pubs@uow.edu.au)

---

# Development and evaluation of a comfort-oriented control strategy for thermal management of mixed-mode ventilated buildings

## Abstract

The paper presents the development, implementation and performance investigation via simulations and experiments of a comfort-oriented control strategy for natural ventilation and mechanical air conditioning management of a mixed-mode building. The proposed comfort-oriented control strategy determines whether it would be possible to operate in natural ventilation mode or in mechanical heating/cooling. The control algorithm calculates first the optimal opening percentage of the windows according to adaptive thermal comfort criteria. If natural ventilation cannot guarantee the thermal comfort requirements and mechanical conditioning is required, the algorithm dynamically optimises the heating or cooling set-point targeting a defined Predicted Mean Vote (PMV) index objective. The performance of the proposed controller was tested via simulations and experiments by using a residential mixed-mode building as a case study. The house features operable windows, a reverse-cycle ducted air conditioner and a comprehensive experimental control and monitoring infrastructure. A comparison with a baseline control strategy was performed to evaluate the comfort and energy performance improvement potential of the proposed control algorithm. The comfort-oriented controller was proven to outperform the baseline controller in terms of maintaining comfort in accordance with targets set by the current comfort standards, such as deviation from a PMV set-point or the middle of the adaptive thermal comfort band. The building energy consumption was also reduced in cooling dominated conditions. The experimental tests demonstrated that this logic can be integrated in an embedded controller, and its performance is in line with the expected one from the simulation results.

## Disciplines

Engineering | Science and Technology Studies

## Publication Details

Fiorentini, M., Serale, G., Kokogiannakis, G., Capozzoli, A. & Cooper, P. (2019). Development and evaluation of a comfort-oriented control strategy for thermal management of mixed-mode ventilated buildings. *Energy and Buildings*, 202 109347-1-109347-16.

# Development and evaluation of a comfort-oriented control strategy for thermal management of mixed-mode ventilated buildings

Massimo Fiorentini<sup>\*a</sup>, Gianluca Serale<sup>b,c</sup>, Georgios Kokogiannakis<sup>a</sup>, Alfonso Capozzoli<sup>b</sup>,  
Paul Cooper<sup>a</sup>

<sup>a</sup> Sustainable Buildings Research Centre (SBRC), Faculty of Engineering and Information Sciences, University of Wollongong, New South Wales, 2522, Australia

<sup>b</sup> Department of Energy (DENERG), TEBE Research group, Politecnico di Torino, Corso Duca degli Abruzzi, 24, 10129 Turin, Italy

<sup>c</sup> CHAOS Lab, Andlinger Center for Energy and Environment, Princeton University, Princeton, NJ, 08544, USA

Declarations of interest: none

\*Corresponding Author: massimo@uow.edu.au

**Abstract:** The paper presents the development, implementation and performance investigation via simulations and experiments of a comfort-oriented control strategy for natural ventilation and mechanical air conditioning management of a mixed-mode building. The proposed comfort-oriented control strategy determines whether it would be possible to operate in natural ventilation mode or in mechanical heating/cooling. The control algorithm calculates first the optimal opening percentage of the windows according to adaptive thermal comfort criteria. If natural ventilation cannot guarantee the thermal comfort requirements and mechanical conditioning is required, the algorithm dynamically optimises the heating or cooling set-point

targeting a defined Predicted Mean Vote index objective. The performance of the proposed controller was tested via simulations and experiments by using a residential mixed-mode building as a case study. The house features operable windows, a reverse-cycle ducted air conditioner and a comprehensive experimental control and monitoring infrastructure. A comparison with a baseline control strategy was performed to evaluate the comfort and energy performance improvement potential of the proposed control algorithm. The comfort-oriented controller was proven to outperform the baseline controller in terms of maintaining comfort in accordance with targets set by the current comfort standards, such as deviation from a PMV set-point or the middle of the adaptive thermal comfort band. The building energy consumption was also reduced in cooling dominated conditions. The experimental tests demonstrated that this logic can be integrated in an embedded controller, and its performance is in line with the expected one from the simulation results.

Keywords: Adaptive thermal comfort; Mixed mode ventilation; Natural ventilation and HVAC control; PMV-based control; Building management systems;

## 40      **Nomenclature**

41     $I_{cl}$  = clothing level index [clo]

42     $wp$  = operable windows' opening percentage level (control action) [%]

43     $k$  = control time step index

44     $M$  = metabolic rate index [met]

45     $mode$  = operating mode

46     $\beta$  = *room* volume air changes per control time-step

47     $\varepsilon_{To}$  = cumulative error from temperature set-point in natural ventilation

48     $\varepsilon_{PMV}$  = cumulative error from PMV set-point in mechanical ventilation

49     $PMV_i$  = indoor Predicted Mean Vote (PMV) index

50     $PMV_{set,c}$  = target PMV in cooling mode

51     $PMV_{set,h}$  = target PMV in heating mode

52     $RH_i$  = indoor relative humidity [%]

53     $T_{m,j}$  = calculated mixed indoor air temperature [°C]

54     $T_a$  = indoor air temperature [°C]

55     $T_{out}$  = outdoor air temperature [°C]

56     $T_o$  = operative temperature [°C]

57     $T_{gi}$  = indoor black globe temperature [°C]

58     $\overline{T_r}$  = calculated indoor mean radiant temperature [°C]

59     $T_{rm}$  = running mean temperature [°C]

60     $T_{AC,set}$  = target air conditioner temperature set-point [°C]

61  $T_{NV,set}$  = target natural ventilation temperature set-point [ $^{\circ}\text{C}$ ]

62  $\theta$  = wind direction [ $^{\circ}$ ]

63  $v_{ar}$  = indoor relative air velocity [m/s]

64  $v_w$  = wind velocity [m/s]

## 65 **1. Introduction and background**

66 Heating and cooling to maintain appropriate thermo-hygrometric conditions in buildings is a  
67 substantial energy end use [1]. Many studies have explored opportunities to reduce energy  
68 consumption for heating and cooling through improvements to the building fabric, more  
69 efficient HVAC equipment, or implementation of intelligent energy management systems  
70 [2,3]. Increasing affordability of electronic componentry has led to an expansion in the  
71 deployment of distributed sensors and controllers in buildings. Combined with improved  
72 computational power in embedded controllers, this has created an opportunity for more  
73 advanced control strategies for the optimisation of energy and comfort in buildings. The  
74 management of these increasingly complex strategies, which may utilise various resources to  
75 optimise for multiple control objectives, is an important challenge.

76 There is a substantial body of literature exploring innovative control logics with a focus on  
77 commercial, institutional or educational buildings. However, fewer studies have focussed on  
78 the use of innovative controls in residential buildings. Building Energy Management Systems  
79 (BEMS) are typically only implemented in non-residential buildings [4]. This is primarily for  
80 economic reasons, as the initial investment for non-residential buildings is generally much  
81 higher than for residential, and it is easier to justify the substantial capital cost of a BEMS.  
82 BEMS allow a significant number of variables to be monitored and for the HVAC parameters  
83 to be dynamically modified [5]. Newer technologies, such as ‘smart thermostats’, are becoming

more common in residential applications. However, these systems are simpler than traditional BEMS, and are only applicable in certain situations. A promising energy management strategy is the automatic windows opening which plays a fundamental role in maintaining suitable indoor comfort conditions in residential buildings [6, 7], but is not typically incorporated into simple control solutions.

### **1.1 Control of mixed-mode buildings**

In mixed mode residential buildings with automated window opening, the mechanical heating and cooling system should be integrated with the window opening controller. The basic concept for these buildings is to maintain a satisfactory indoor environment by alternating between and combining natural and mechanical systems to reduce the use of the HVAC system throughout the year [8]. Depending on the location, natural ventilation can substantially reduce energy consumption in a building [9,10], and the control of natural ventilation operation plays an important role in achieving this reduction, either by being manually operated and reliant on human behaviour [11] or automated with simple or complex control algorithms [12,13]. Natural ventilation has additional benefits in certain circumstances, including improved indoor air quality (when the building is located in a non-polluted area) and a reduced risk of overheating in summer [14].

Although many climatic zones are suitable for the utilisation of natural ventilation in buildings, in particular in Australia [15] the literature reports relatively few cases of buildings that fully exploit an optimised natural ventilation strategy. This is often due to the lack of an optimised automated control system for the windows openings, and the inability of the occupants to open and close the windows in the right conditions to exploit the natural ventilation potential [16].

When a building is operating in natural ventilation mode, it is important to control the window opening percentage in order to manage air velocity in the space. Air velocity can strongly affect

an occupants' perceived comfort and cause local discomfort due to draughts [17]. Raja et al. [18] highlighted the direct positive relationship between an occupants' willingness to interact with the natural ventilation control of their office space, and their thermal comfort. Providing occupants with manual control over window opening, or relying on predefined opening schedules has been shown to lead to an increased risk of thermal discomfort, and to energy wastage, which can negate the energy savings achievable from natural ventilation [19,20].

In cases where a control system is in place for the operation of windows, the integration and coordination of the operable windows with the conventional HVAC system is challenging [21,22].

Assessing the best logic for mixed-mode buildings is non-trivial, since factors influencing comfort in natural and mechanical ventilation have to be considered simultaneously, as well as the response of the building to various forcing variables (outdoor temperature, humidity, wind speed and direction). Mixed-mode buildings typically feature a high-level controller that defines whether the building can operate in natural ventilation or must rely on mechanical air conditioning based on a set of predefined rules. A lower level controller will then either determine the window opening percentage or activate the mechanical system. The indoor temperature set-point for the mechanical systems is then generally fixed and pre-defined, and the heating or cooling control algorithms work independently from the window opening controller logic.

The assessment of occupants' thermal comfort in mixed-mode buildings is also a challenging task [23–25]. Rijal et al., [19] found that thermal conditions in mixed-mode buildings were generally controlled as if they were in naturally ventilated buildings, but with the provision for cooling if needed, rather than as in normal air-conditioned buildings. The well-known Predicted Mean Vote (PMV) can only be used to evaluate the microclimatic conditions of conditioned environments, while the adaptive thermal comfort theory is only applicable to



passive naturally ventilated buildings. Traditional thermostatic controllers regulate the active system of the building based on indoor dry-bulb temperature measurements. Controlling internal temperature based on adaptive thermal comfort theory requires measurement of a greater number of parameters, for instance Mean Radiant Temperature [26] or feedback from the occupants [27], in order to compute comfort indexes in real time and thereby optimise the building operation.

## **1.2 Recent advances in control algorithms for mixed-mode buildings**

There are several examples of recent research focused on control strategies for mixed mode ventilation buildings. Drake et al., [8] assessed the thermal sensations of occupants of two mixed-mode office buildings, i.e., one educational and one commercial. The control logic implemented operated a fixed set-point for the air conditioning system (24 °C) with a large deadband ( $\pm 1.5$  °C). The controllers switched-over to natural ventilation mode only when external weather conditions or indoor thermal temperatures met pre-defined conditions (e.g., outdoor air temperature below a specific threshold). Fu and Wu [28] stated that occupant comfort must be the primary objective of a controller in hybrid ventilated buildings. Psomas et al. [14] conducted a simulation study on the automated control of a single-family house with operable openings. The study defined a methodology and a framework of how to simulate a ventilative cooling algorithm of a window system in a building simulation performance tool.

Several studies have identified an approach using Model Predictive Control (MPC) more suitable to capture the complex dynamics of mixed-mode buildings. May-Ostendorp et al. [29] and Zhao et al. [30] formulated a Model Predictive Control problem in Matlab for regulating mixed-mode buildings, represented by simulations in EnergyPlus. Hu and Karava [31,32] conducted a simulation study based on model-based controller formulation. They found that the non-linearities introduced by the natural ventilation airflow network required the adoption

of a numerical optimization, i.e., a Particle Swarm Optimisation algorithm, which has implications for the computational performance of an embedded controller. Spindler and Norford [33,34] presented different configurations of a short term predictive controller acting as a supervisory control layer for optimising the internal air temperature set-point of a mixed-mode ventilated institutional building. The optimal solution was provided by a model-based controller, using both building and airflow network models tailored with data gathered in field. The control input influenced only the flow rate of outdoor air entering in the building using automated openings or mechanical fans, with the regulation of the active HVAC system identified as an area for further research. In 2018, Chen et al. [35] further demonstrated the effectiveness of MPC algorithms for the regulation of hybrid ventilated buildings. This study was based on numerical simulations implementing a non-linear MPC using an artificial neural network to model the dynamic behaviour of a building. These studies have all demonstrated the potential effectiveness of MPC regulation for building performance. Challenges remain in the detailed definition of a control oriented model for the implementation of MPC in real buildings, as well as in creating a controller that can be employed in a large number of buildings.

Barbadilla-Martín et al. [36] used an adaptive comfort algorithm to recursively adjust the indoor air temperature set-point (and the controller deadband) of 11 mixed-mode office spaces in Spain. A large dataset was analysed in this paper, which outlined the complications inherent in defining a suitable baseline for calculating the energy savings achievable by means of experimental tests with different controllers. A limitation in this study was that although the windows were manually operated, this study considered the investigated offices as a mixed-mode building by limiting the control logic to the definition of the mechanical HVAC system set-point.

### **1.3 Current issues in assessing thermal comfort in mixed-mode buildings**

A number of strategies have been employed in previous literature for the management of mixed-mode buildings, without a clear consensus on the optimal method. Practitioners therefore typically use a tailored approach in devising regulation strategies for mixed-mode buildings, as a result of the lack of standard methods. Standards still conservatively categorize mixed-mode buildings as part of fully mechanically conditioned environments. This constrains mixed-mode buildings to operate in a restrictive PMV range, and therefore a comfort-based control algorithm for the regulation of the indoor conditions is not able to maximize the energy saving. Many authors have addressed this lack in the regulation of the conditions in mixed-mode buildings by providing long-term comfort assessments [37,38], comparing in-situ measurements and questionnaires to thermal comfort standards [39] and analysing the occupants' response to conditions occurred during the mechanical and natural ventilation operating modes of the building [40]. Luo et al. [41] explored this issue, and found that adaptive comfort theories better predict the thermal sensation of mixed-mode buildings occupants, compared with the steady state PMV model. A guideline for integrating adaptive thermal comfort requirements within traditional PMV theory can be found in the standard ISO 7730 (ATG) of Netherlands [42].

#### **1.4 Goals and framework of the paper**

The current paper presents a comfort-oriented control strategy, which aims at maximising indoor thermal comfort by adapting the controller objective to the relevant thermal comfort theory for the chosen ventilation mode. The adaptive thermal comfort theory was employed to optimise the operation of the natural ventilation mode operation, while the PMV index was used for periods of mechanical heating and cooling operation. The ASHRAE Standard 55 was considered as the reference for the calculation of the control targets [43].

The controller was developed using affordable electronic devices to demonstrate that this solution could be scalable at residential level. In order to reduce the energy demand, natural ventilation through opening of the windows was selected as the preferred building operating mode. When the building operated in this mode, a simplified air flow network was solved to predict the air temperature at the next control time step, and to determine to optimal window opening percentage for thermal comfort. If opening the windows was not able to guarantee the satisfaction of the adaptive thermal comfort bounds, mechanical heating or cooling was activated. In this scenario, the controller optimised the set-point of the air conditioning system by calculating the temperature at which the desired PMV level would be achieved.

The controller's performance was tested using numerical simulations and experimental tests. A case study residential building was used for both the simulations and the experimental tests. A dedicated simulation platform that linked building energy performance simulation software and an external controller at each time-step was developed for this purpose. This was used to benchmark the performance of the comfort-oriented control strategy against a baseline controller under the same operating conditions.

The same control algorithms were also implemented in a low-cost controlling hardware, and integrated into the control system of the case study house. This provided a practical demonstration of the integration of the logic in an embedded controller, as well as providing experimental validation of the simulation results through comparison of the performance of the comfort-oriented control strategy against a baseline controller.

## 2. Methodology

### 2.1 Baseline controller

The adaptive controller developed in this study was compared with a baseline competing algorithm. The baseline algorithm was the controller originally implemented in the case study building that was employed in the current study (see Section 3). The implementation of the baseline controller was based on rules sourced from building operation specifications defined by a building mechanical engineering consultant.

The baseline controller switched between natural and mechanical ventilation, and determined the window opening percentage, based on the measurement of the outdoor dry-bulb temperature  $T_{out}$  as follows:

- When the outdoor temperature was between 20°C – 24°C, the windows were fully open;
- If the outdoor temperature was between 18°C – 20°C and 24 °C - 26°C windows were open at 50%, only if heating or cooling mode are not already active. These partial openings do not allow the full benefits of natural ventilation to be exploited. For instance, night cooling can be effectively used in the summer time by completely opening the windows when the outdoor temperature reaches values within the 24 – 26 °C band.
- When the outdoor temperature was below 18°C the heating mode was activated and the air conditioner was configured with a constant indoor temperature set-point of 20°C. The heating mode was then deactivated when the outdoor temperature reached 20°C. The cooling mode was activated when the outdoor temperature exceeded 26°C and deactivated at 24°C, with an indoor temperature set-point of 24°C.

A graphical representation of this control logic is shown in Figure 1.

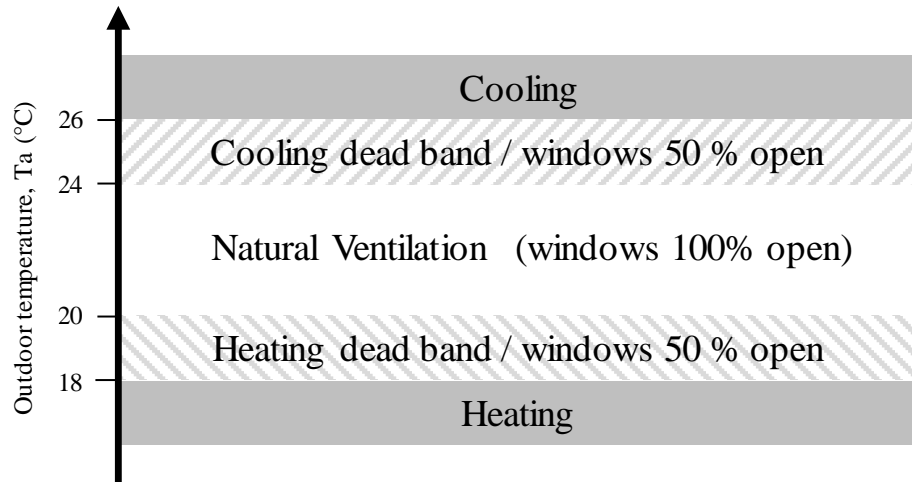


Figure 1: Baseline controller operating mode decision logic.

## 2.2 Formulation of the comfort-oriented control strategy

Multiple factors beyond dry bulb temperature affect perception of thermal comfort, therefore a simple thermostat based control will not always be sufficient to capture the required information to maintain comfort in a mixed-mode building. The goal of the proposed comfort-based controller algorithm for window openings was to improve the occupants' comfort satisfaction in accordance with the limits and comfort indexes used in current thermal comfort standards [43].

The proposed comfort-oriented control strategy would generally be active only when the house is occupied, because windows will typically be shut when the building is unoccupied due to security concerns (precluding natural ventilation), and mechanical conditioning will not typically be active for energy saving purposes. Occupancy detection could be implemented in the controller by using presence/motion sensors or manual user inputs. However, since this study includes experimental tests that are affected by a number of unmeasured disturbances, we decided to remove the additional uncertainty resulting from unknown occupant behaviour. The experimental campaign was therefore undertaken with the house unoccupied to achieve

equivalent and comparable results.

The control of the mixed-mode ventilation was achieved in two steps. Firstly, the operating mode for the current control time-step was determined (either natural ventilation or mechanical conditioning). Secondly, either the optimal set-point of window opening percentage or the air conditioner temperature set-point was defined, depending on the operating mode that was set from the first step. The controller aimed to predict the outcome of all the possible subsequent control actions and then select the optimal solution.

Current comfort standards are either applicable to fully naturally ventilated (e.g. adaptive thermal comfort) or to fully mechanically ventilated buildings (e.g. PMV method), since there is no defined standard that is applicable to a mixed-mode building. The absence of defined standards applicable to mixed mode buildings is reflected in the proposed controller logic, as it integrates two different comfort theories for managing a mixed-mode building. During the controller development, the principles of the adaptive comfort theory were used to determine if the building could use natural ventilation, as well as the set-point temperature that had to be maintained through the opening of windows. If natural ventilation could maintain the indoor conditions within the prescribed constraint, it was always preferred since it exploits the climatic potential and reduces the building energy consumption. The controller logic allows operable windows to be operated at steps of opening of 20% (this percentage could be reconfigured depending on the window type). When natural ventilation was not possible and mechanical heating or cooling was required, the PMV index was adopted as an objective for the controller to indicate occupant comfort. PMV is currently the most recognized thermal comfort indicator for fully mechanically ventilated buildings. A schematic of the control process is presented in Figure 2.

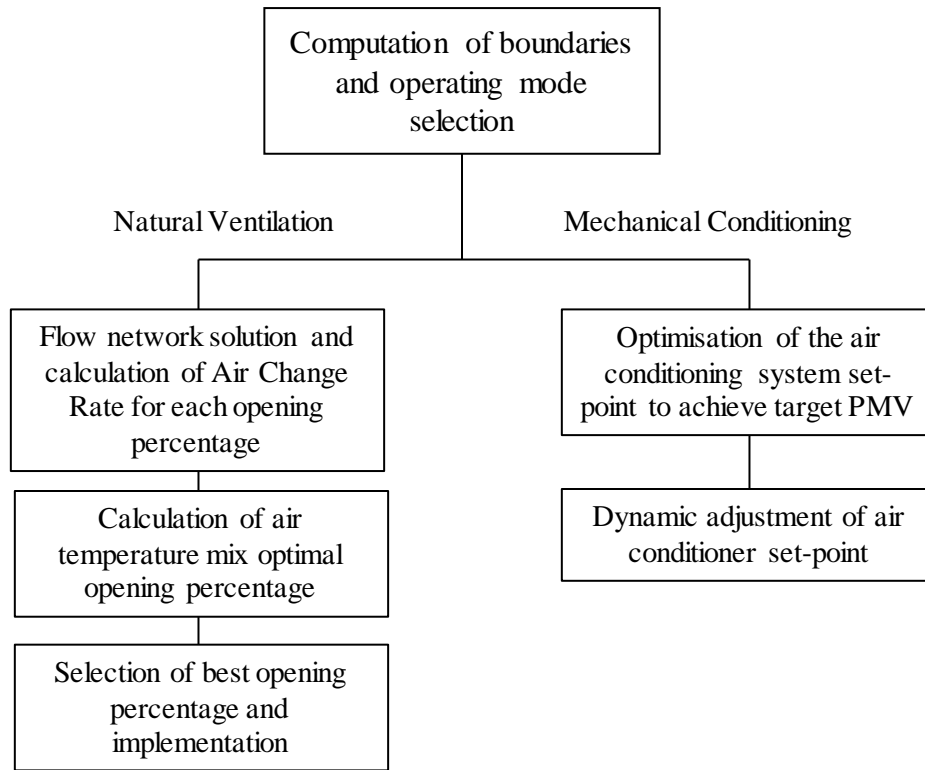


Figure 2: Process schematic for comfort-oriented control.

The set-points and boundaries used in the proposed controller logic are not fixed thresholds before the deployment of the controller, but they are daily re-calculated values capable of considering the variation of an occupant's acceptability bands of adaptive thermal comfort. Figure 3 shows the variation of the set-point and the relative bounds for seven days of operations.



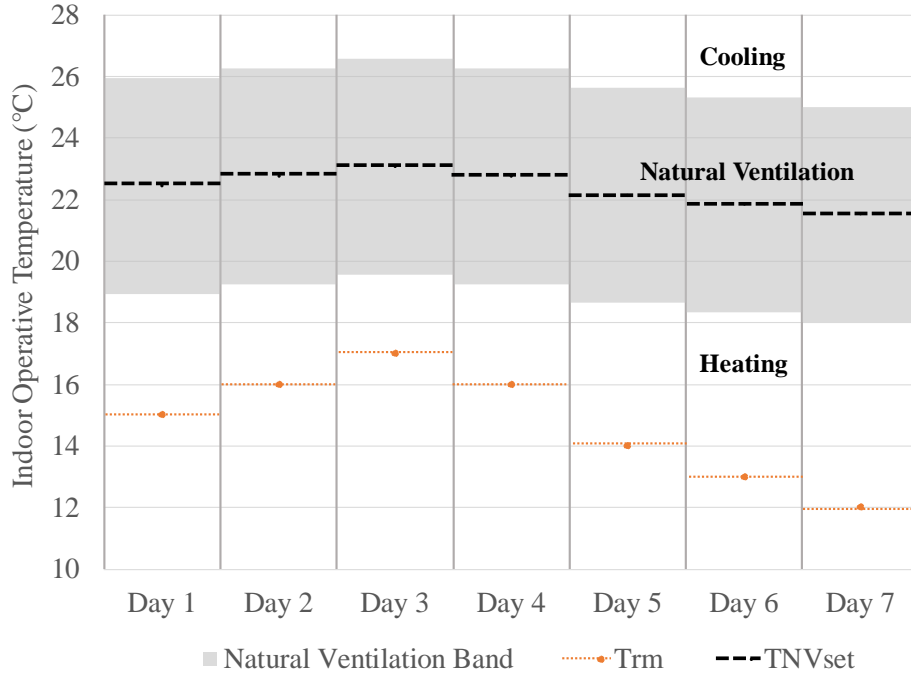


Figure 3: An example illustrating the evolution of the comfort-oriented controller set-points over time. The grey area represents the periods during which the controller will select the natural ventilation mode.

### 2.2.1 Operating mode selection: Natural ventilation or Mechanical Heating or Cooling

The upper and the lower temperature boundaries of the thermal acceptability limits retrieved from adaptive thermal comfort standard (ASHRAE 55 [43]) were calculated dynamically in order to select the mode of operation. The running mean temperature,  $T_{rm}$ , was calculated each day as a function of the average temperatures of the previous seven days. These data were monitored by the weather station described in Section 3.2 and located just outside the case study house. The upper and the lower boundaries of the adaptive thermal comfort band represent the daily limits in which the natural ventilation mode can be activated, and they were calculated as in Eq.1.

$$\begin{cases} T_{NV,max} = 0.31 \cdot T_{rm} + 21.3 \\ T_{NV,min} = 0.31 \cdot T_{rm} + 14.3 \end{cases} \quad (1)$$

The set-point selected for the thermal regulation to be achieved in natural ventilation mode was evaluated as the mean value of the adaptive thermal comfort temperature limits, as presented

313 in Eq.2. This operation was performed daily, at midnight.

$$314 \quad T_{NV,set} = (T_{NV,min} + T_{NV,max})/2 \quad (2)$$

315 An example of the evolution of the indoor set-point temperature in natural ventilation mode is  
316 shown in Figure 3 over a period of seven days. It can be observed that the set-point changed  
317 dynamically according to the running mean temperature.

### 318 **2.2.2 Natural ventilation: flow network solution and calculation of Air Change Rate** 319 **for each opening percentage**

320 The optimal opening percentage of the windows was calculated based on the solution of a  
321 simplified flow network considering only wind-driven ventilation (buoyancy effects were not  
322 considered). The controller first calculated the surface-averaged wall pressure coefficients  
323 using polynomial interpolation of the curves recommended by ASHRAE Fundamentals  
324 Handbook [44], and from the measured wind speed and direction. The opening area of the  
325 windows was then calculated as in Eq. 3. The area of each window  $i$  open at a percentage level  
326  $j$  was calculated as:

$$327 \quad A_j = [1 - \cos(\text{asin}(l_c \cdot wp_j))] \cdot L \cdot H \quad (3)$$

328 Where  $l_c$  is the length of the window chain,  $wp_j$  is the window opening percentage at each level  
329  $j$ ,  $L$  and  $H$  are the length and width of each window as reported in Table 1.

330 The solution of the flow network allowed the controller to compute the predicted number of  
331 volume air changes per control time-step ( $\beta_j$ ), at each opening level  $j$ . This value is numerically  
332 limited between 0 and 1, where 1 represents the full air exchange.

### 333 **2.2.3 Natural ventilation: calculation of air temperature mix and selection of optimal** 334 **opening percentage**

335 In natural ventilation mode, the controller regulated the internal operative temperature resulting

from the mixing of indoor and outdoor temperature by adjusting the opening percentage of the operable windows. The comfort based controller aimed to predict the indoor operative temperature at the next control time-step (considered one hour long) for each possible operable window opening position.

Since the mean radiant temperature will change more slowly compared to the indoor air temperature, and generally a significant variation of the internal surface wall temperature would not be expected to occur during a control time step, it was assumed to be constant for the calculation of the operative temperature at the next time step.

The predicted indoor air temperature  $T_{a,j}$  was therefore the only necessary parameter to be calculated for the next control time step;  $T_{a,j}$  was evaluated as a straightforward mixing of the two air volumes at indoor and outdoor temperature, as shown in Eq.4.

$$T_{a,j} = (1 - \beta_j) \cdot T_a + \beta_j \cdot T_{out} \quad (4)$$

Where  $T_a$ , and  $T_{out}$  are the current internal and external air temperatures, and  $\beta_j$  the aforementioned predicted number of volume air changes. The operative temperature  $T_{o,j}$  was then calculated as the mean between the indoor air and mean radiant temperature.

The optimal window opening position ( $j^*$ ) was the one that minimises the distance between the predicted indoor operative temperature at the next control time step and the natural ventilation set-point, as per Eq. 5.

$$j^* = \operatorname{argmin} (|T_{o,j} - T_{NV,set}|) \quad (5)$$

## 2.2.4 Mechanical ventilation: optimisation of the air conditioning system set-point

In the case where the indoor conditions were outside the adaptive thermal comfort limits, mechanical heating or cooling was activated. In this operating mode, the set-point for the

internal air temperature was selected by reversing Fanger's PMV comfort index. The house HVAC system configuration allowed only the indoor air temperature to be used as adjustable input variable. The other environmental variables affecting the PMV index (i.e., internal mean radiant temperature, air velocity, and relative humidity) were monitored and affect the comfort dynamics as measured disturbances. Significant changes of the measured disturbances were not expected in short span represented by the control time step. The optimal temperature set-point was calculated as the dry-bulb temperature that would result in a PMV level at the border of a "comfort class B" range ( $PMV = \pm 0.5$ , representing  $PMV_{set,h}$  and  $PMV_{set,c}$ ) in accordance with ref. [45]. The set-point for the indoor air temperature was calculated iteratively using the bisection method.

In the present experimental study, the tests were conducted assuming a clothing index equal to  $I_{clo} = 1$  clo (i.e. typical heating season clothing [46]). The metabolic rate was set to  $M = 1.2$  met, which is the value indicated for dwelling sedentary activity [46]. These values could be adjusted depending on the specific application or in accordance with the occupants' requirements. In the simulations performed in the various seasons, the clothing index was considered to be equal to 1 clo in winter, 0.5 clo in summer and 0.75 clo in the middle seasons.

## 2.3 Description of the case study building

An experimental test of the developed controller was completed using a case study high performance single family dwelling, namely the Team UOW “Illawarra Flame” house that won the 2013 Solar Decathlon China competition. This building features a mixed-mode ventilation system that utilises both natural ventilation and mechanical heating or cooling. The controller of the house was original a simple control logic commonly used in Australia to handle natural and mechanical ventilation as described in Section 2.1. This was the baseline controller used for comparison in this study to test the performance of the new comfort-oriented control strategy. The house was located at the Innovation Campus of the University of Wollongong in Wollongong, New South Wales, Australia. External and internal views of the house are shown in Figure 4. The building is located in Climate Zone 5 - warm temperate in the Australian National Construction Code climate classifications. This climatic zone is characterised by low temperature difference between night and day, mild winter conditions, comfortable outdoor temperatures during swing seasons (spring and autumn), and summer conditions with high temperatures and moderate humidity. These weather conditions are suitable for exploiting natural ventilation benefits, especially during the swing seasons.



Figure 4: Illawarra Flame house at Innovation Campus, Wollongong, Australia

The overall thermal resistance of the opaque components of the building (ceiling, walls, and floors) was approximately  $6.0 \text{ m}^2 \text{ K}^{-1} \text{ W}^{-1}$ . Windows are timber-framed and characterised by a Solar Heat Gain Coefficient (SHGC) equal to 0.3 and a U-Value lower than  $1.5 \text{ W m}^{-2} \text{ K}^{-1}$ . A degree of thermal mass was added to the lightweight timber structure with a  $2.2 \text{ m} \times 3.2 \text{ m} \times 0.1 \text{ m}$  thick concrete panel added to an internal living room wall. A shading system in the form of fixed slatted timber screen was installed on the east and west facades of the house to reduce excessive solar heat gains. The indoor environments can be conditioned using an air-based system equipped with a reversible heat pump. The nominal heating and cooling design capacity of the mechanical system is 7 kW.

One of the key targets of the original Solar Decathlon project was to achieve net-zero energy consumption throughout the year. To achieve this target, a number of energy efficient passive and active measures were applied to the house, including the exploitation of natural ventilation. The house was a suitable case study for testing a mixed-mode ventilation building as the building controller has the flexibility to be interfaced to each individual HVAC component, as well as with external sensors. The window opening regulation is adjustable at 1% intervals allowing effective control of natural ventilation flow rates. The mechanical heating or cooling is provided by a 7 kW conventional reverse cycle ducted air conditioner, with a temperature set-point resolution of  $1^\circ \text{C}$ . The set-point is determined by regulating a high level controller. The HVAC component operates as a single-zone system that is entirely regulated by the thermostat located in the living room. This is a traditional set-up for residential dwellings in the area of the study.

A plan view of the house layout highlighting the operable windows locations (positions A to E at lower level and windows H at upper level) is presented in Figure 5. The operable windows are of various typologies and sizes. The existing controller only enables a simultaneous

operation of all the windows together. A summary of the windows characteristics that are used in Eq. 3 is reported in Table 1.

Table 1. Illawarra Flame house – windows characteristics.

Window	Type	L [m]	H [m]	l <sub>c</sub> [m]
A	Awning	0.80	1.50	0.30
B	Casement	0.54	1.50	0.30
C	Casement	0.54	1.40	0.30
D	Awning	0.40	1.40	0.30
E	Awning	0.40	1.40	0.30
H	Awning	1.30	0.30	0.30

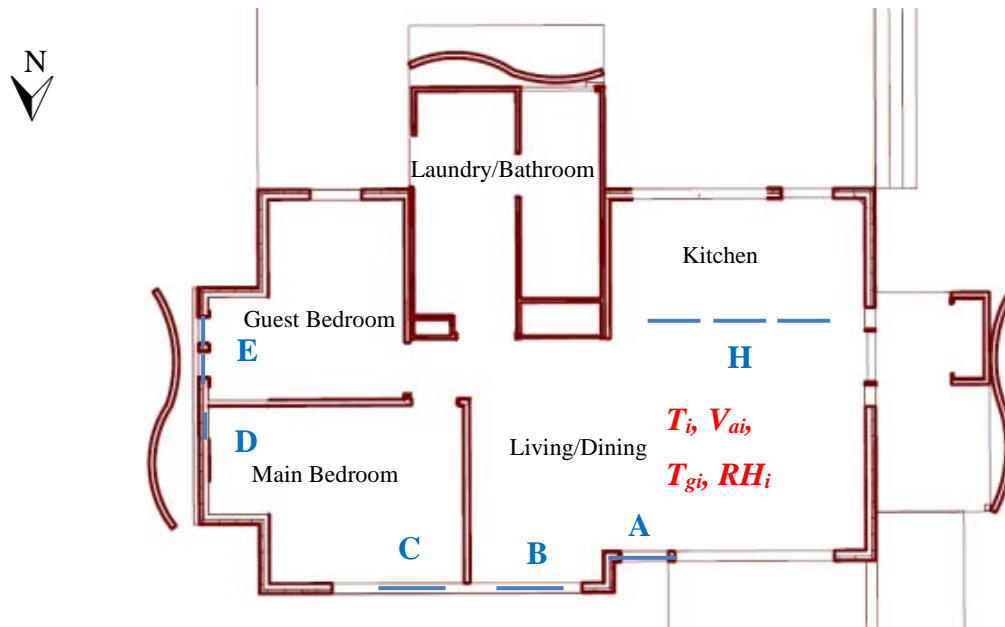


Figure 5: Illawarra Flame house – Operable windows are shown in blue. The controller and its sensing unit (using a Raspberry Pi and relevant sensors that are discussed in Section 3.2) is shown in red.

### 2.3.1 Building Management Control System (BMCS) architecture and integration

The control system of the Illawarra Flame house was designed to accommodate the objectives and constraints of the overall Solar Decathlon project, and to be capable of controlling lighting systems, operable windows and the complex HVAC system. The BMCS is also capable of monitoring temperatures, energy consumption, electricity generation and flow rates, and can

effectively report this information to the user via a graphical interface. The system is based on Clipsal C-Bus components.

A supervisory BMCS (Tridium Niagara JACE) was integrated with the local low level control system, to act as a data logger and a gateway to various communication languages, such as Modbus and oBIX [47] networks.

The JACE controller also has the capability to over-ride the local controller of the reverse-cycle air conditioning unit, utilising a Modbus gateway, allowing the control system to dynamically change the operation mode of the HVAC system, the temperature set-point and the fan speed. The controllers of windows located at lower level (i.e., windows A to E), which adjust the window opening percentage, are also connected to the JACE controller via Modbus. The architecture of the BMCS is shown in Figure 6 and is discussed below.

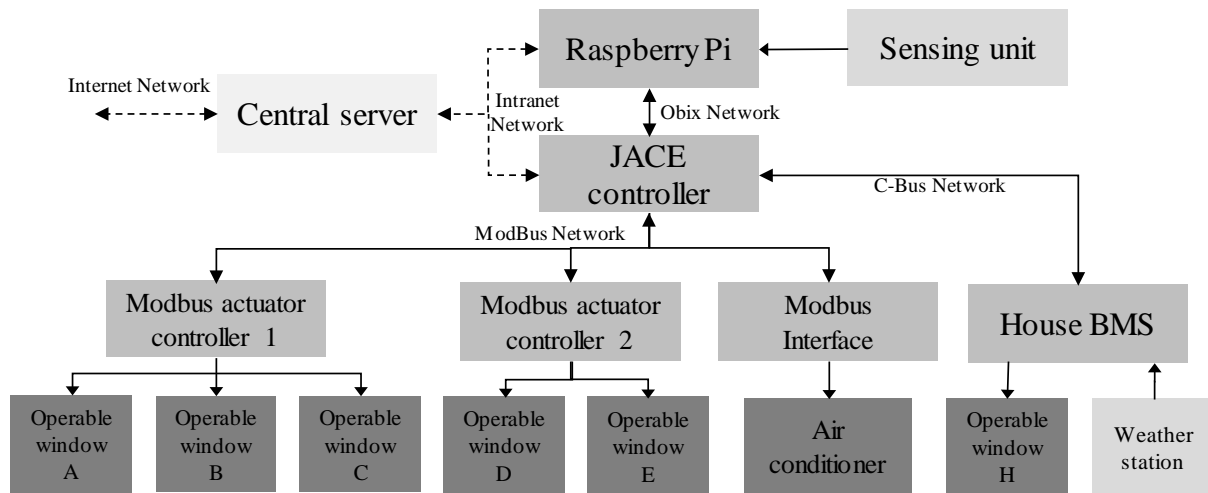


Figure 6: BMCS system integration, windows and air conditioning control schematic.

One of the goals of the current paper is to highlight the potential to run smart control algorithms on affordable control processors. A Raspberry Pi 3 model B was selected for this purpose. The Raspberry Pi is one of the most widespread single-board computers with a 1.2GHz quad-core ARMv8 processor and 1 GB of integrated RAM. The market offers many alternatives that are equivalent to this controller. The control algorithm was implemented using Python, which is a



license-free software. The sensors attached to the Raspberry Pi and the control algorithm were interfaced to the JACE controller using an oBIX network interface (Figure 7).



Figure 7: Window actuator (Window A) and JACE controller.

The python control algorithms implemented on the Raspberry pi are the same implemented in the simulation platform described in Section 2.4, with some of the variables of the array  $\mathbf{x}^*(k)$  pre-processed on-board from the real-time measurements and with the outputs  $\mathbf{u}^*(k)$  directly controlling the windows opening, air conditioning system set-point and operating mode.

### 2.3.2 Monitoring instrumentation

The outdoor weather conditions were monitored using a Davis Vantage Pro II Weather station, integrated through an RS232 connection to the C-Bus and JACE control units. The weather parameters considered by the control algorithm are: outdoor temperature (nominal accuracy  $\pm 1$  °C, range -40 to 65 °C), global horizontal solar radiation (nominal accuracy  $\pm 5$  % of full scale, range up to 1800 W/m<sup>2</sup>), wind speed (nominal accuracy  $\pm 0.9$  m/s, range 1 to 89 m/s), and wind direction (nominal accuracy  $\pm 3^\circ$ ). The weather station was located on the roof of the controlled house (approximately 4 m height). Since the distance between the wind speed sensor and the opening height of the upper windows was less than 1 m, the measured wind speed values were not adjusted for height differences.

The indoor conditions were monitored using a sensing unit equipped with low cost sensors, directly connected to the Raspberry Pi unit (Figure 8). The sensors used were those required for the determination of the PMV index and their characteristics are listed in Table 2. The location of the Raspberry Pi controller and the sensor units are highlighted in Figure 5. All the sensors were placed at 1 m height.

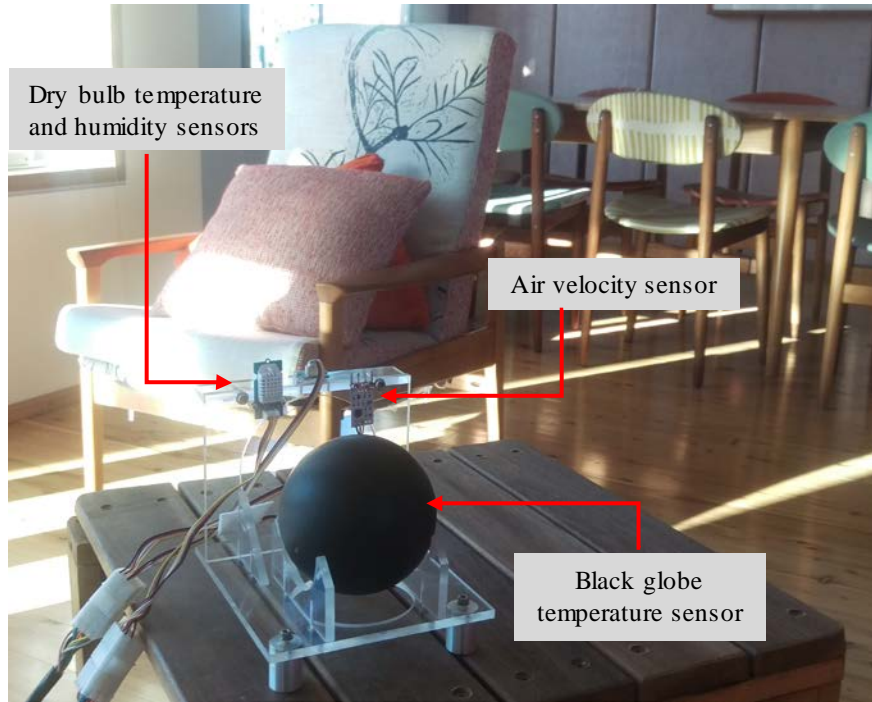


Figure 8: Raspberry Pi sensing unit

Table 2: Raspberry Pi sensor list

Sensor	Variable	Accuracy	Type
Indoor air temperature, Indoor relative humidity	$T_a$ $RH_i$	$\pm 0.3^\circ\text{C}$ $\pm 2\%$	Thermistor - digital
Black globe temperature	$T_{gi}$	$\pm 0.3^\circ\text{C}$	Thermistor in a 100 mm diameter black copper sphere
Air velocity	$v_w$	Not provided	Hot wire anemometer - analog

The sensors and the Raspberry Pi acquisition chain were calibrated against a high accuracy sensors system, which met the requirements of ASHRAE 55 and ISO 7726:1988 standards. The details of this system are presented in Table 3.

480

Table 3: Reference sensors list

Sensor	Range	Accuracy	Type
Indoor air temperature	0 – 50°C	20°C = $\pm 0.04^\circ\text{C}$ 30°C = $\pm 0.05^\circ\text{C}$	RTD PT100
Relative humidity	0 – 95 %	0-60% = $\pm 2.5\%$ 0-80% = $\pm 3.0\%$	HUMICAP
Black globe temperature	0 – 50°C	$\pm 0.5^\circ\text{C}$ or $\pm 0.4\%$ reading	T-Type thermocouple in a 40 mm diameter black copper sphere
Air velocity	0.05 – 2.50 m/s	$\pm 3\%$ reading $\pm 1\%$ full scale range	Hot wire anemometer - omnidirectional probe tip

481

482 The sensors allow the measurement of the variables that are required to calculate the PMV  
483 index and the adaptive thermal comfort band. These measurements were either direct (e.g.  
484 indoor air temperature, relative humidity, indoor air velocity) or determined using intermediate  
485 calculations. The indoor mean radiant temperature was evaluated with a black globe  
486 thermometer, and from the measurements of indoor air temperature and indoor air velocity to  
487 remove convective effects. The experiments were undertaken with control and measurement  
488 time steps both being equal to 5 minutes. During the experimental campaign, the internal doors  
489 remained open, and the controller regulated the spaces as a single-zone.

#### 490 **2.4 Simulation Platform for Controller Benchmarking**

491 In order to benchmark the performance of the baseline and the adaptive comfort controller, an  
492 ad-hoc simulation platform was developed, building on the previous work by some of the  
493 current authors [22,48]. Simulations were deemed necessary for validation of the experimental  
494 results, allowing detailed comparison of the performance of the comfort-oriented controller  
495 under the same boundary conditions as the baseline controller.

496 To achieve a time-step coupling between a building energy performance simulation software  
497 and a complex controller, the Building Control Virtual Test Bed (BCVTB) tool [49] was used

as an interface. We have modified the standard ESP-r building simulation software code to enable sending the array of measurements,  $\mathbf{x}(k)$ , necessary for the controller to compute the optimal natural or mechanical ventilation strategy via the BCVTB socket, and to receive the required inputs,  $\mathbf{u}(k)$ , from the controller to operate the building systems (windows and mechanical heating/cooling). The information sent from ESP-r was pre-processed by the BCVTB, in order to be able to send computed variables (such as  $T_{rm}$ ) in the array of measurements  $\mathbf{x}^*(k)$  to the controller, which was programmed in Python. A schematic of this software integration is presented in Figure 9.

The controller input array was  $\mathbf{x}^*(k) = [T_i, RH_i, v_w, \overline{T_r}, T_a, RH_o, T_{rm}, \theta, I_{cl}]$  and the output array was  $\mathbf{u}(k) = [j^*, T_{AC, set}, mode]$ . The indoor air velocity, which was used by the controller to calculate the optimal air temperature set-point when in mechanical ventilation mode, was assumed to be constant and equal to 0.2m/s for PMV calculations [43].

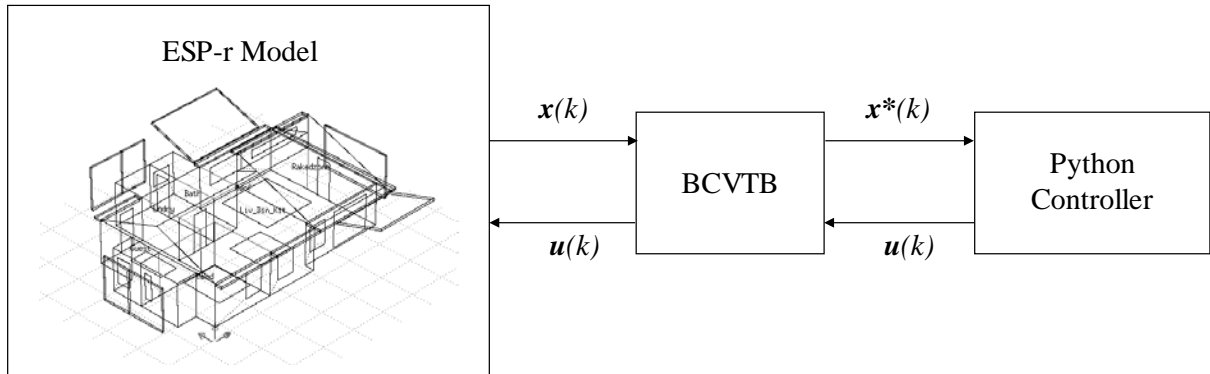


Figure 9: Simulation Platform software integration using a model of the case study building.

### 3. Results and Discussion

#### 4.1 Simulation Results

A simulation was completed for both controllers using International the Weather for Energy Calculations (IWEC) file over a summer month (January), a winter month (July) and an autumn month (April). A portion of the results for each month is reported in Figure 10, Figure 11, and Figure 12 respectively. A complete summary of the results is provided in Section 4.3.

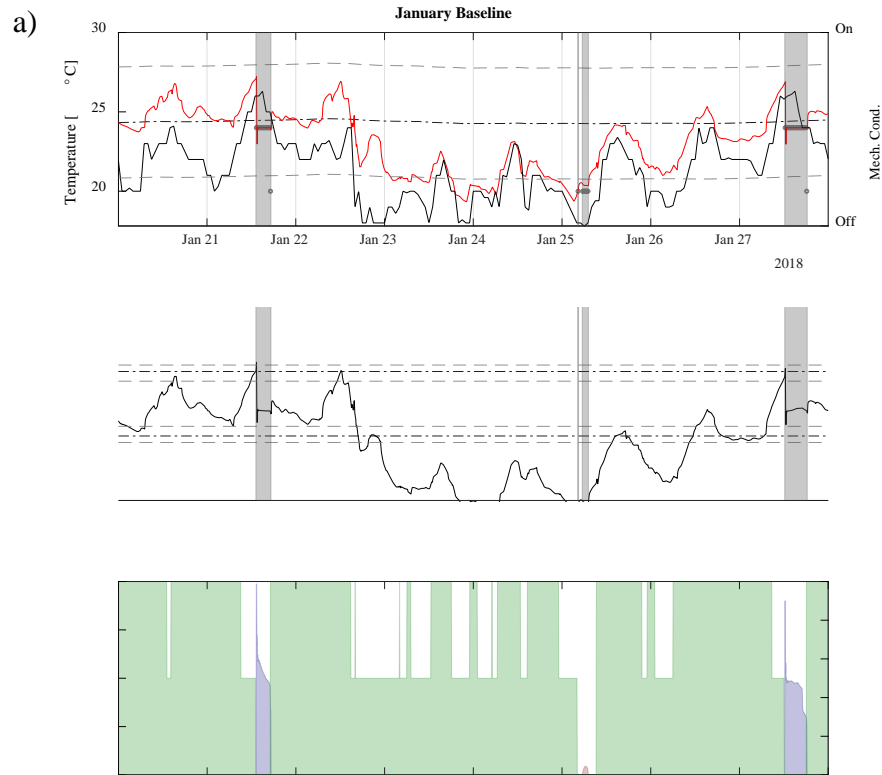
Each figure contains three sub-figures: the first reports the indoor and outdoor temperature conditions, air conditioning system set-point and the adaptive thermal comfort boundaries; the second one displays the associated PMV values and the boundaries of ISO Class B acceptability range; and the last presents the control inputs to the house (heating, cooling, or opening percentage of windows). The shaded areas of the first two subplots of each figure highlight the periods when mechanical conditioning was operating.

In both cases shown in Figure 10 and Figure 11, the comfort-oriented controller outperformed the baseline controller in terms of both maintaining comfort and reduced energy consumption. In Figure 10a, the windows are either fully open or partially open for the majority of the time. This is due to baseline controller calculating the operation of the windows based on the outdoor temperature only. In the situation shown, the windows are kept open even when it would not be advisable to do so, as the indoor temperature is at the lower end of the comfort band and the outdoor air is cooler (e.g. between the 23<sup>rd</sup> and 26<sup>th</sup> of January). This resulted in indoor conditions outside the adaptive thermal comfort band, on the cold side, while in natural ventilation mode. For the same period the windows operated considerably less frequently when the comfort-oriented controller was employed, shown in Figure 10b, especially in the middle of the period presented.

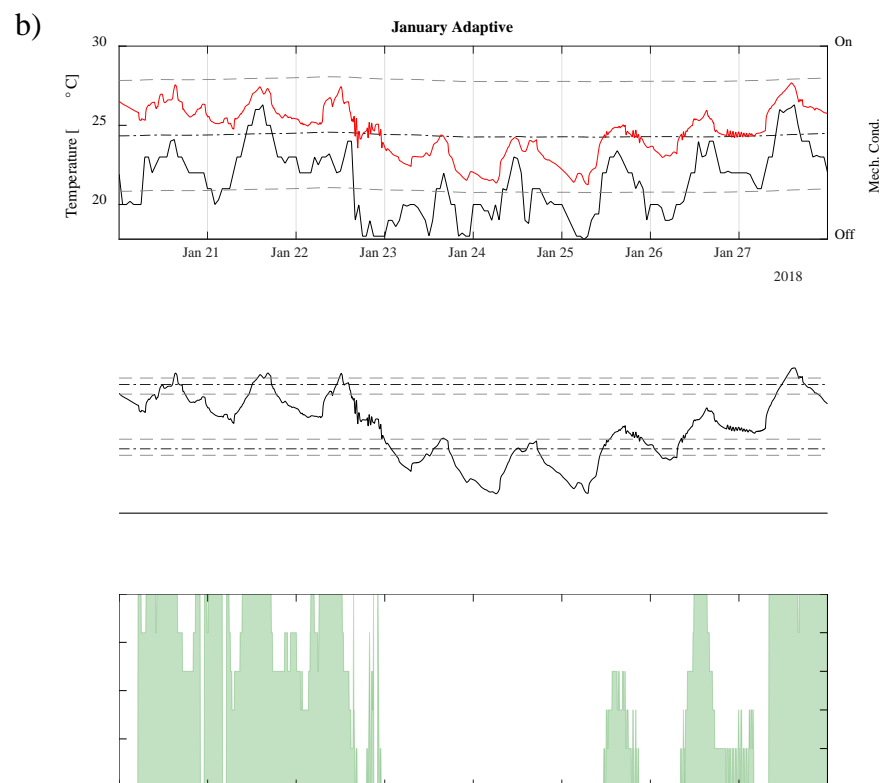
538 During the period shown, the baseline controller activated the cooling mode on two occasions,  
539 despite the indoor air temperature remaining within the comfort range, while the comfort-  
540 oriented controller did not utilise mechanical conditioning for the entire period.

541 A similar behaviour in natural ventilation mode can also be noticed during the middle season  
542 in April (Figure 11 – 14<sup>th</sup> and 15<sup>th</sup> of April), during which the baseline controller tended to  
543 overcool the building towards the bottom of the comfort range. Furthermore, when heating and  
544 cooling was needed, the comfort-oriented controller imposed a higher indoor set-point  
545 temperature compared to the baseline controller in order to better achieve the PMV target.

546



547



548

549

550

Figure 10: Simulation results, January, Sydney. a) baseline controller; b) comfort-oriented controller.

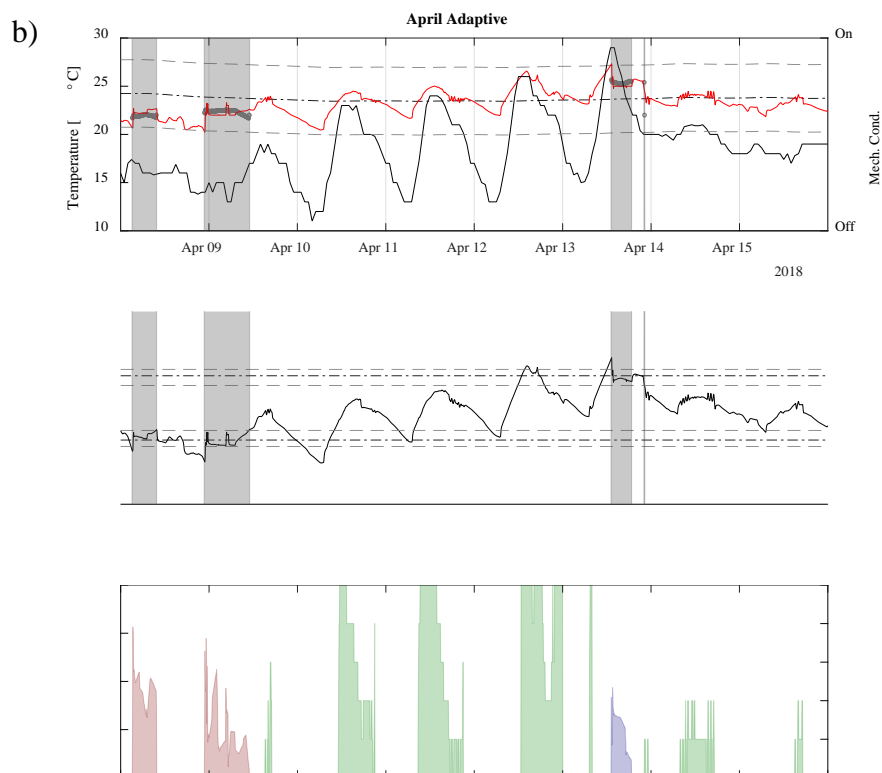
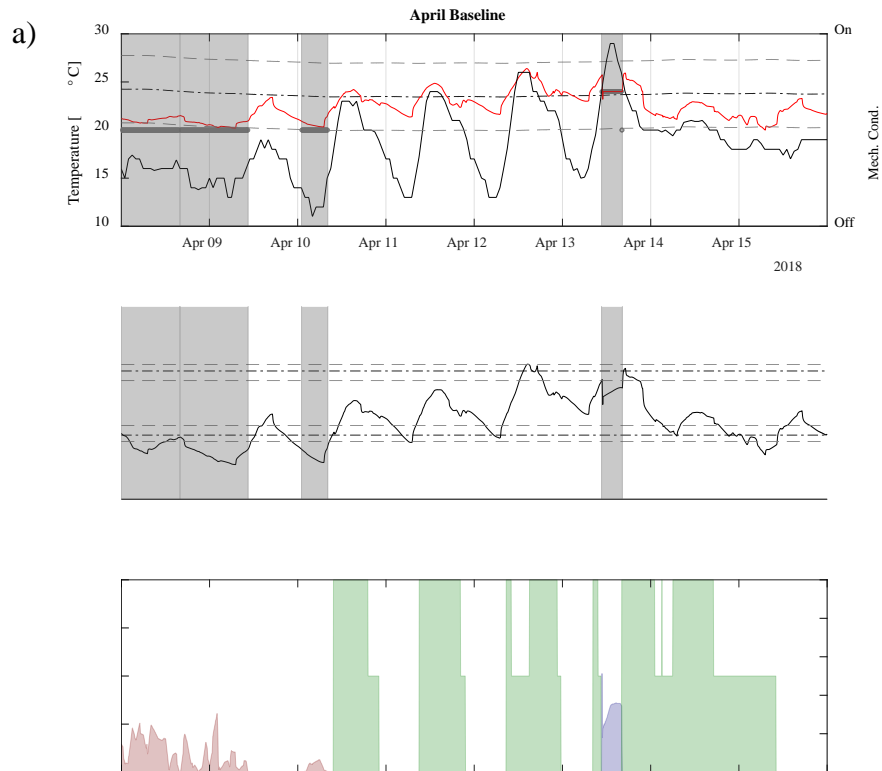


Figure 11: Simulation results, April, Sydney. a) baseline controller; b) comfort-oriented controller.



555 In winter conditions, mechanical heating was generally needed in the case study building, as  
556 shown in both Figure 12a and Figure 12b. Despite maintaining a relatively constant  
557 temperature, as shown in Figure 12a, the baseline controller was not able to ensure that the  
558 PMV level remained within the recommended range, due to the other dynamically changing  
559 variables included in the PMV calculation. The comfort-oriented controller was able to manage  
560 this issue by dynamically varying the heating set-point (e.g. 12<sup>th</sup> of July) to maintain a more  
561 constant PMV, as shown in Figure 12b. Consequently, there was an improvement of occupants'  
562 thermal comfort with just a slight increase of the overall energy consumption (approximately  
563 6%, as presented in Table 4). Quantitative simulation results are summarised and discussed in  
564 Section 4.3 and more specifically in Table 4, together with the experimental results of this  
565 study.

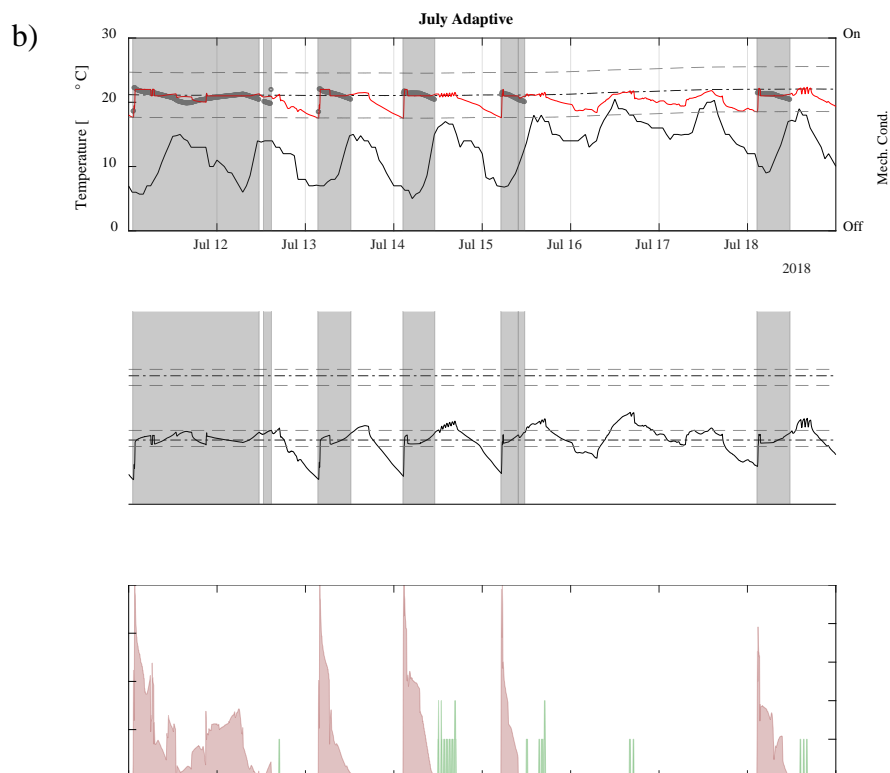
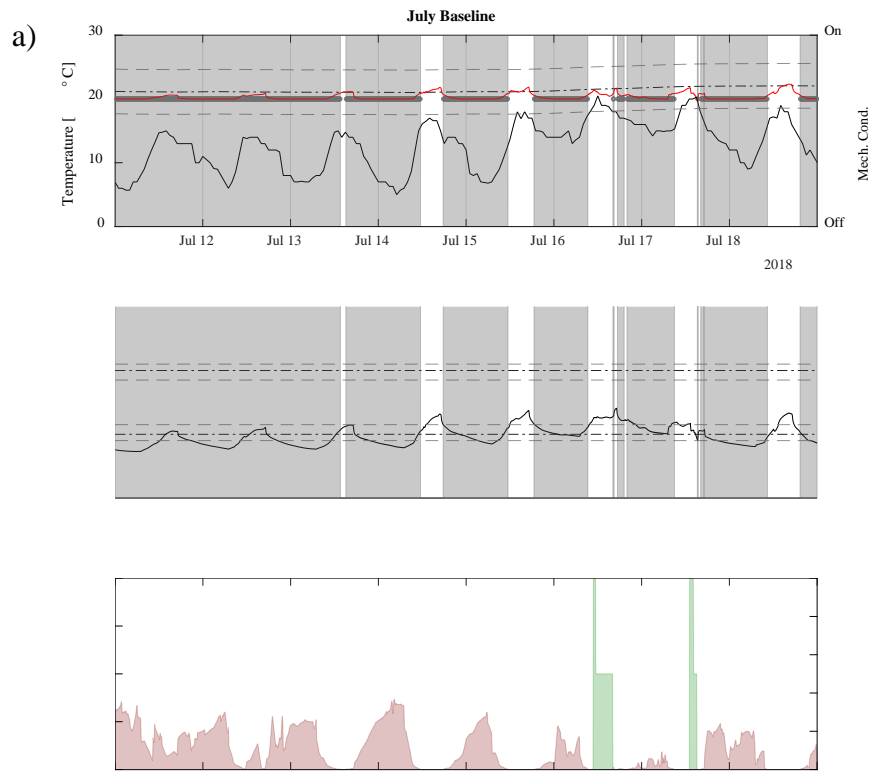


Figure 12: Simulation results, July, Sydney. a) baseline controller; b) comfort-oriented controller.

## 4.2 Experimental Results

Both the baseline and the comfort-oriented control strategies were tested on the Illawarra Flame house using the infrastructure presented in Section 3.2. The baseline controller was tested between the 21<sup>st</sup> and the 23<sup>rd</sup> of April 2018 and the results are reported in Figure 13. The comfort-oriented controller was tested between the 26<sup>th</sup> and the 29<sup>th</sup> of May 2018 (Test 1) and the 30<sup>th</sup> and 31<sup>st</sup> of May 2018 (Test 2), and the results are presented in Figure 14 and Figure 15 respectively (the test was interrupted on 29<sup>th</sup> of May due to other issues with the house). Figures are organised in the same way as that used for the simulations.

Although the baseline controller was generally capable of maintaining the indoor operative temperature within the adaptive thermal comfort range, as shown in Figure 13 the temperature was mostly close to the lower limit of the adaptive acceptability range, for example between 11 am and 11 pm on the 21<sup>st</sup> of April. This result is also observed in the January and April simulation results. This lower internal temperature often resulted in heating being required shortly afterwards.

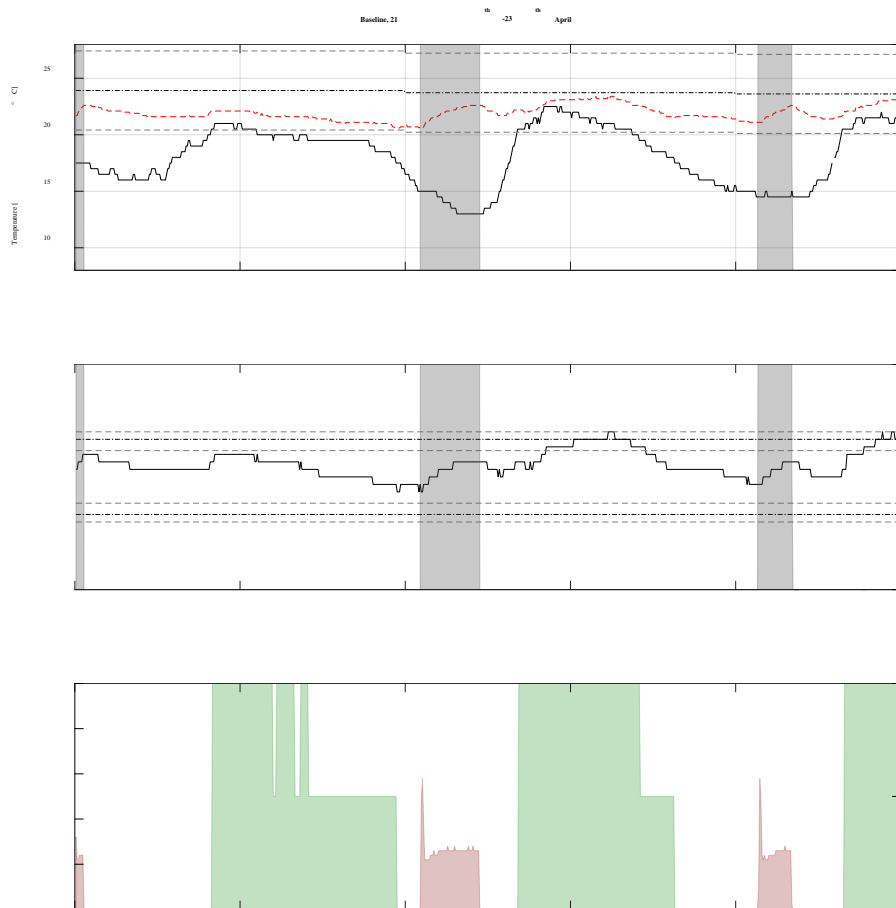


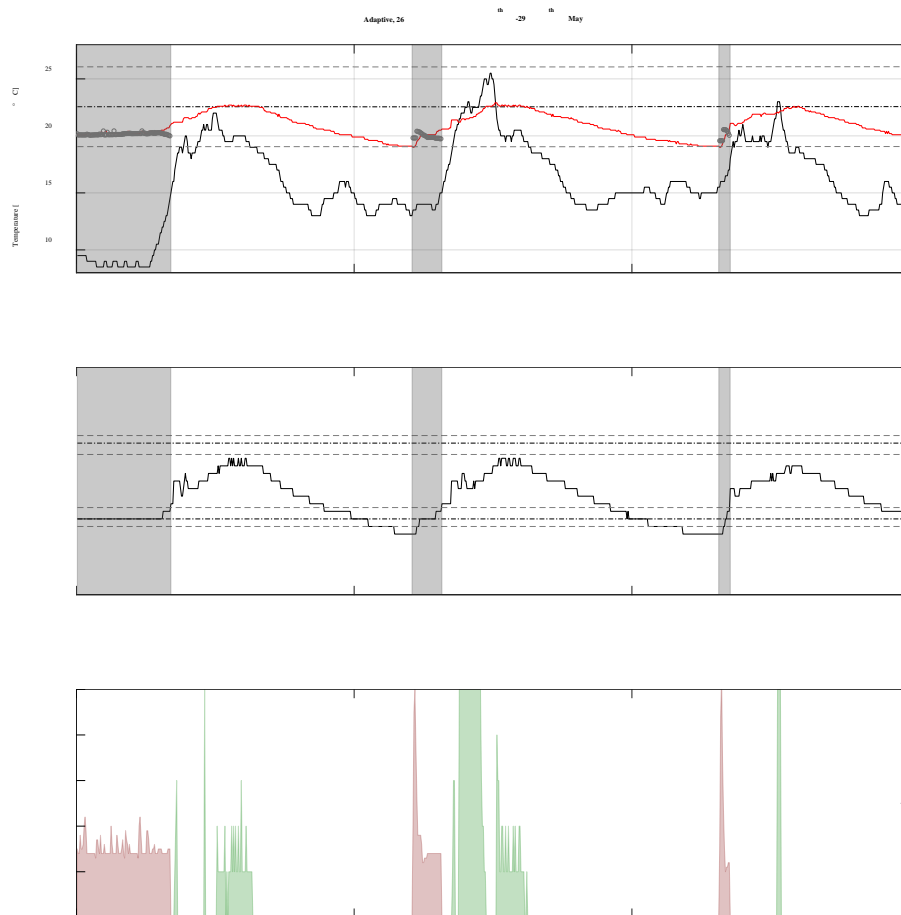
Figure 13: Baseline controller: experimental test, 21<sup>st</sup>-23<sup>th</sup> April 2018

Whilst the baseline control logic used both the outdoor and indoor temperatures as input parameters, these variables were treated as independent. This leads to less optimal thermal comfort levels than could have been achieved if the windows were kept shut during the above example on the 21<sup>st</sup> of April. It also resulted in higher energy consumption, due to the need for mechanical heating overnight.

The PMV levels recorded during this test are reported in the lower subplot of Figure 13. It should be re-iterated that PMV is only indicative of comfort for periods of mechanical ventilation. The indoor air temperature is the only parameter affecting the PMV directly manipulated by the mechanical heating system. Given that the lower the set-point of indoor air temperature, the lower the energy use for space heating is, the PMV should be maintained as

596 close as possible to the lower acceptable bound during the heating season. For a comfort Class  
597 B building this lower acceptable PMV level is equal to -0.5. In Figure 13 the PMV levels are  
598 considerably above the minimum required level for a Class B building, and exceed 0 during  
599 the periods of mechanical heating. The increase of PMV to levels above 0 was due to the  
600 internal dead-bands of the heat pump controller, which resulted to indoor temperatures around  
601 22°C even if the set-point during the heating operation was 20°C.

602 The results for the comfort-oriented controller test presented in Figure 14 refer to relatively  
603 warm days where cooling was generally needed during the day and heating during the night,  
604 similarly to the period of the test with the baseline controller. During this testing period, the  
605 indoor temperature remained within the adaptive comfort band. The test started in relatively  
606 cold conditions, with the controller in heating mode for the first hours of the test. During these  
607 first hours, the controller adjusted the heat pump set-point to maintain a constant PMV value.



608

609 Figure 14: Comfort-oriented controller: experimental test during relatively warm days, 26<sup>th</sup>-  
610 29<sup>th</sup> May 2018.

611 When natural ventilation mode operated (e.g. around 12:00 of the 26<sup>th</sup> of May), the controller  
612 effectively modulated the window opening percentage to keep the indoor temperature steady  
613 at the defined set-point in the middle of the adaptive comfort band. The windows were opened  
614 to regulate the indoor temperature for cooling purposes during the day of the 26<sup>th</sup> of May.  
615 During the second day (i.e., 27<sup>th</sup> of May), mechanical heating was needed for the first part of  
616 the day. Once the external conditions were appropriate, the system switched to natural  
617 ventilation mode and opened the window because the outdoor temperature was higher than the  
618 indoor. When the indoor temperature reached the natural ventilation set-point  $T_{NV,set}$ , the  
619 outdoor temperature was higher than the indoor one and the controller closed the windows to  
620 avoid overheating (27<sup>th</sup> of May, 12:00). When the outdoor temperature decreased towards the

end of the afternoon of the same day, the controller started to modulate the windows opening to provide a minimal amount of natural cooling to keep the indoor temperature close to the set-point. During the third day (i.e., 28<sup>th</sup> of May), the windows were only open when the outdoor temperature sharply increased during the afternoon for a short amount of time (28<sup>th</sup> of May, 12:00), in an attempt to bring the indoor temperature closer to the middle of the adaptive comfort band set-point.

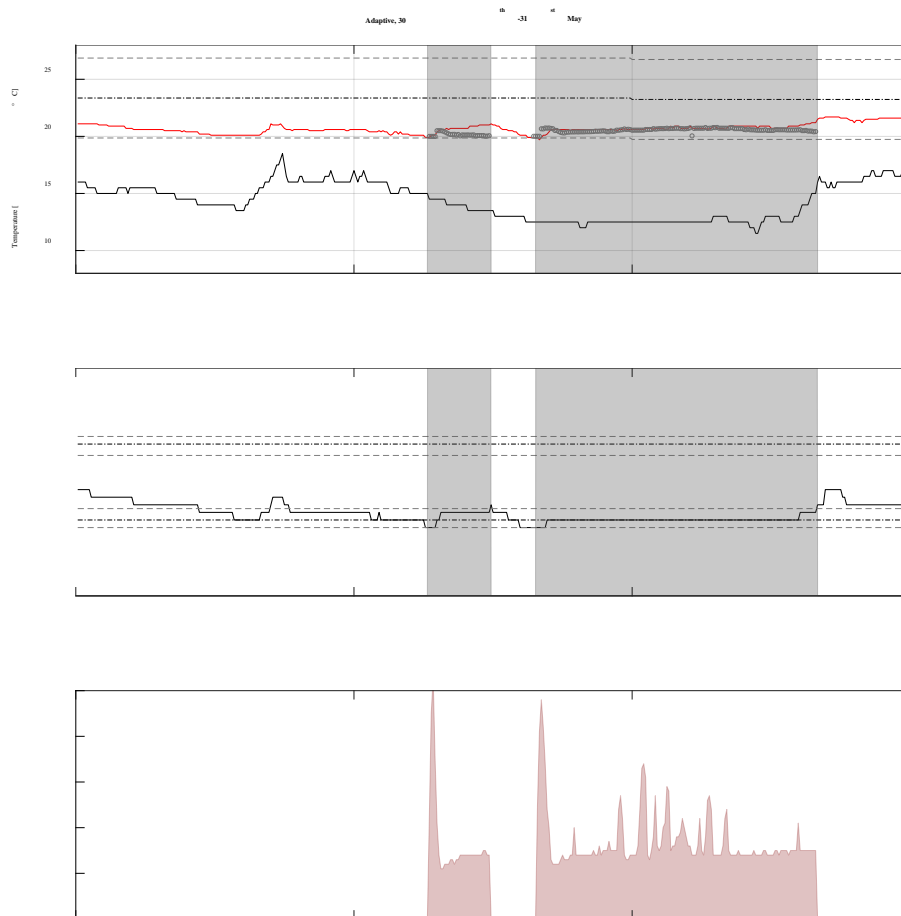


Figure 15: Comfort-oriented controller: experimental test during relatively cold days, 30<sup>th</sup>-31<sup>st</sup> May 2018.

The results presented in Figure 15 refer to relatively cold days, when mechanical heating was mostly needed. Observing the upper and lower subplots, it can be seen that the controller dynamically adjusted the heat pump set-point to keep a constant PMV value and better control the heating request. In the third subplot it can be seen that during the first heating operation the

PMV slightly increased above the required set-point, and the controller responded by reducing the temperature set-point to restore the PMV to the correct level. During the second heating period, the controller maintains the PMV level constant at the set-point for the entire period.

### 4.3 Results summary

The simulated and experimental tests conducted in this study provide an effective demonstration of the possibility to integrate an advanced control logic for mixed mode ventilation on an embedded controller. An indication of the performance in terms of maintaining comfort during the tests has been shown by calculating the cumulative deviation of either:

- i) the indoor operative temperature from the middle of the adaptive thermal comfort band, during natural ventilation operation mode, or;
- ii) the indoor PMV from the objective level of  $\pm 0.5$  of the boundary of a comfort Class B building, during mechanical ventilation mode.

In both cases deviation below or above this objective is equally penalised as loss of thermal comfort.

The specific Key Performance Indicators, measuring a deviation from the ideal temperature or PMV set-points, used to evaluate the controller performance in terms of satisfaction of occupants' comfort requirements were:

$$\varepsilon_{PMV,heat} = \frac{\sum_{k=0}^{N_m} |PMV_{i,k} - PMV_{set,k}|}{N_{heat}} \quad (6)$$

$$\varepsilon_{PMV,cool} = \frac{\sum_{k=0}^{N_m} |PMV_{i,k} - PMV_{set,k}|}{N_{cool}} \quad (7)$$



$$\varepsilon_{T_o} = \frac{\sum_{k=0}^{N_{NV}} |T_{o,k} - T_{NV\_set,k}|}{N_{NV}} \quad (8)$$

Where  $N_{heat}$  and  $N_{cool}$  are the total number of hours where the mechanical heating/cooling system mode was active (respectively in heating or cooling) and  $N_{NV}$  is the total number of hours where the system operated in natural ventilation mode. Each indicator accounted only the instances when their respective operating mode was active Eq. 6 and Eq. 7 refer to Fanger's theory for a comfort Class B building, while Eq. 8 refers to the adaptive comfort band from ASHRAE 55.

The amount of time the building was operating in free running mode is also presented in these two tables (FR in Table 4 and Table 5), as a percentage of the total time (not a fraction of the time in which the system was in the specific operating mode) the building was operating without additional heating or cooling, i.e. when in natural ventilation mode, the controller defined the windows position " $wp = 0$ " as the optimal decision for ensuring adaptive thermal comfort or when in mechanical conditioning mode, the controller selected an optimal PMV-based set-point that is reachable without activating the heat-pump.

Table 4 reports the primary outcomes of the numerical simulations. The daily average energy needed for the heating and cooling periods is also reported by assuming ideal systems.

668

Table 4: Key performance indicators for the simulations.

Month	Controller	NV (FR) [-]	Heating (FR) [-]	Cooling (FR) [-]	$\varepsilon_{To}$ [°C/ $\Delta t$ ]	$\varepsilon_{PMV,heat}$ [-/ $\Delta t$ ]	$\varepsilon_{PMV,cool}$ [-/ $\Delta t$ ]	Heating [kWh/day]	Cooling [kWh/day]
Jan	Baseline	78.1%	10.5%	11.3%	1.508	0.608	0.731	0.385	5.726
		(0%)	(7.8%)	(0.2%)					
	Adaptive	88.7%	2.5%	8.7%	1.101	0.077	0.064	1.260	1.748
		(42.7%)	(0.01%)	(1.2%)					
Apr	Baseline	37.5%	58.7%	3.7%	1.318	0.273	0.327	0.652	1.171
		(0%)	(49.9%)	(0.1%)					
	Adaptive	90.0%	2.8%	7.0%	1.053	0.076	0.065	0.905	0.797
		(67.6%)	(0.02%)	(3.6%)					
Jul	Baseline	3.3%	96.6%	0%	1.054	0.142	N/A	12.734	0
		(0%)	(14.3%)	(0%)					
	Adaptive	51.2%	48.7%	0%	1.603	0.057	N/A	13.519	0
		(46.8%)	(1.8%)	(0%)					

669

670 Table 5 refers to the outcomes of the experimental tests. The tests were performed in a period  
671 when mechanical cooling was not necessary. Outcomes carried out experimentally have the  
672 limitations of comparing experimental tests undertaken at different time periods.

673

Table 5: Key performance indicators for the experimental tests.

Period	Controller	NV (FR) [-]	Heating (FR) [-]	$\varepsilon_{To}$ [°C/ $\Delta t$ ]	$\varepsilon_{PMV,heat}$ [-/ $\Delta t$ ]
21-23 Apr	Baseline	48.1% (0%)	51.9% (39.6%)	2.64	0.60
26-29 May	Adaptive	84.0% (71.9%)	2.8% (0%)	1.51	0.03
30-31 May	Adaptive	58.9% (58.4%)	48.7% (0%)	2.63	0.02

674

The internal dead-bands of the air conditioning system baseline controller allowed the system to heat the building 2 °C above the set-point. The resulting PMV was therefore always significantly above -0.5 and even above 0 for a large fraction of the time. This effect was limited by the comfort-oriented control strategy, which adjusted the heat pump set-point to modulate the heating delivery and stopped the heat pump operation when the PMV reached a level higher than the adaptive comfort requirements. When analysing the cumulative deviations in Table 5, it can be seen that, during mechanical operation hours, the comfort-oriented control strategy performed better than the baseline. During the natural ventilation hours, the Adaptive Comfort Controller in Test 1 (26<sup>th</sup>-29<sup>th</sup> May) outperformed the baseline Controller, since it could utilise the outdoor conditions to properly maintain the indoor conditions close to the required set-point. Optimising the mixing of outdoor air with the indoor to only occur when favourable, and by controlling the exchange rate, made it possible to ensure the indoor temperature was as close as possible to the set-point, with minimal oscillations around it. During the second testing period (30<sup>th</sup>-31<sup>st</sup> May), the comfort-oriented control strategy had an approximately similar performance to the baseline Controller. This is due to the very different weather conditions during the two tests. In fact, during the second test, the windows were never opened by the comfort-oriented control strategy, as the indoor air temperature was lower than the target temperature, but the outdoor temperature was always even lower than the indoor air temperature.

#### **4. Conclusions**

The current paper proposed a comfort-oriented control strategy to manage a mixed-mode ventilation residential building. A residential building with operable windows, a reverse-cycle ducted air conditioner and comprehensive experimental control and monitoring infrastructure

was used to experimentally and numerically test the performance of the proposed controller in comparison to a baseline one.

The proposed comfort-oriented control strategy acted on two control levels, where the higher level assessed the possibility to operate in natural ventilation mode based on the boundaries of the ASHRAE 55 adaptive thermal comfort model, and the lower level optimised the equipment operation depending on the chosen operating mode. If natural ventilation mode was selected from the higher level, the operation of the natural ventilation mode was optimised on the embedded controller, using the wind speed and direction measurements and the indoor and outdoor temperatures. A simplified airflow network of the building was solved in real time to predict the temperature of the air mix, to determine the window opening percentage that will more closely track the temperature target. If mechanical heating or cooling was selected, the optimal set-point of the air-conditioner was dynamically calculated by the controller, finding the indoor air temperature that would lead to the desired PMV level.

Benchmarking the performance of a controller is difficult via only experiments, as the results are limited by the comparison of outcomes measured at different times. For this reason, a building performance simulation model of the case-study building was developed using ESP-r. The baseline and the comfort-oriented control strategy were coupled at time step level to the building simulation model. Numerical simulations proved the effectiveness of the comfort-oriented control strategy in all seasons in terms of maintaining comfort in accordance with targets set by the current comfort standards, such as deviation from a PMV set-point or from the middle of the adaptive thermal comfort band. The building energy consumption was also reduced in cooling dominated conditions.

The comfort-oriented control strategy developed for this study was also experimentally compared with the standard baseline controller, and despite the limitations of comparing experimental tests that were undertaken at different time periods, it was shown that the comfort-

oriented control strategy can outperform the baseline one, with the results being in accordance to those from the simulations. When in natural ventilation mode, the comfort-oriented control strategy better managed the opening of the windows, more closely tracking the middle of the adaptive comfort band when compared to the baseline controller. Furthermore, in mechanical conditioning mode, selecting the air temperature set-point with the control objective on the target PMV allowed the comfort-oriented control strategy to deviate less from the desired PMV level.

The present approach represents a reliable, affordable, and effective solution to deal with mixed-mode buildings. Compared to alternative model-based approaches it requires a significantly reduced fine-tuning effort enabling the present methodology to be easily generalized to other buildings and climates.

Future work should focus on improving the controller performance using a multi-zone regulation configuration instead of the existing single-zone, or alternative comfort models can be used to define the controller objectives. This could include including suing comfort metrics which are able to assess the users' thermal comfort based on local phenomena (e.g. higher local air speeds), as well as include local discomfort drawbacks, such as the draught risk, in the controller's objectives.

## **Acknowledgement**

The initial research in this paper was partly supported by the Australia-Germany Research Cooperation Scheme, a joint initiative of Universities Australia and the German Academic Exchange Service (DAAD).

## References

- [1] D. Kolokotsa, D. Rovas, E. Kosmatopoulos, K. Kalaitzakis, A roadmap towards intelligent net zero- and positive-energy buildings, *Sol. Energy*. 85 (2011) 3067–3084. doi:10.1016/j.solener.2010.09.001.
- [2] E. Mills, *Building Commissioning: A Golden Opportunity for Reducing Energy Costs and Greenhouse Gas Emissions*, 2009.
- [3] G. Serale, M. Fiorentini, A. Capozzoli, D. Bernardini, Model Predictive Control ( MPC ) for enhancing buildings and HVAC systems energy efficiency : problem formulation , applications and opportunities, *Energies*. 11 (2018) 1–33.
- [4] H.T. Haider, O.H. See, W. Elmenreich, A review of residential demand response of smart grid, *Renew. Sustain. Energy Rev.* 59 (2016) 166–178. doi:10.1016/j.rser.2016.01.016.
- [5] D. Kolokotsa, K. Gobakis, S. Papantoniou, C. Georgatou, N. Kampelis, K. Kalaitzakis, K. Vasilakopoulou, M. Santamouris, Development of a web based energy management system for University Campuses: The CAMP-IT platform, *Energy Build.* 123 (2016) 119–135. doi:10.1016/J.ENBUILD.2016.04.038.
- [6] R. Markovic, E. Grintal, D. Wölki, J. Frisch, C. Van Treeck, Window opening model using deep learning methods, *Build. Environ.* 145 (2018) 319–329. doi:10.1016/j.buildenv.2018.09.024.
- [7] M. Santamouris, F. Allard, *Natural ventilation in buildings: a design handbook*, James and James (Science Publishers) Ltd, London, 1998.
- [8] S. Drake, R. De Dear, A. Alessi, M. Deuble, S. Drake, R. De Dear, A. Alessi, M.D. Occupant, S. Drake, R. De Dear, A. Alessi, M. Deuble, *Occupant comfort in naturally*

769 ventilated and mixed-mode spaces within air-conditioned offices, *Archit. Sci. Rev.* 53  
770 (2010) 297–306. doi:10.3763/asre.2010.0021.

771 [9] K. Niachou, S. Hassid, M. Santamouris, I. Livada, Comparative monitoring of natural ,  
772 hybrid and mechanical ventilation systems in urban canyons, *Energy Build.* 37 (2005)  
773 503–513. doi:10.1016/j.enbuild.2004.09.016.

774 [10] X. Shao, X. Li, X. Ma, C. Liang, Multi-mode ventilation : An efficient ventilation  
775 strategy for changeable scenarios and energy saving, *Build. Environ.* 115 (2017) 332–  
776 344. doi:10.1016/j.buildenv.2017.01.032.

777 [11] S. Manu, C. Patel, R. Rawal, G. Brager, Occupant feedback in air conditioned and  
778 mixed-mode office buildings in India, in: *Proc. 9th Wind. Conf. Mak. Comf. Relev.*,  
779 n.d.: pp. 306–319.

780 [12] L.E. Thomas, Shifting the norm - towards effective mixed mode buildings, in: *30th Int.*  
781 *Plea Conf.*, Ahmedabab: pp. 1–8.

782 [13] J.C. Salcido, A. Abdul, R.R.A. Issa, From simulation to monitoring: Evaluating the  
783 potential of mixed-mode ventilation (MMV) systems for integrating natural ventilation  
784 in office buildings through a comprehensive literature review, *Energy Build.* 127  
785 (2016) 1008–1018. doi:10.1016/j.enbuild.2016.06.054.

786 [14] Ventilative cooling through automated window opening control systems to address  
787 thermal discomfort risk during the summer period: Framework, simulation and  
788 parametric analysis, *Energy Build.* 153 (2017) 18–30.  
789 doi:10.1016/J.ENBUILD.2017.07.088.

790 [15] M. Fiorentini, F. Tartarini, L. Ledo Gomis, D. Daly, P. Cooper, Development of an  
791 enthalpy-based index to assess climatic potential for ventilative cooling of buildings:  
792 An Australian example, *Appl. Energy.* (2019). doi:10.1016/j.apenergy.2019.04.165.

- 793 [16] K. Huang, G. Feng, H. Li, S. Yu, Opening window issue of residential buildings in  
794 winter in north China : A case study in Shenyang, *Energy Build.* 84 (2014) 567–574.  
795 doi:10.1016/j.enbuild.2014.09.005.
- 796 [17] H.B. Rijal, P. Tuohy, M.A. Humphreys, J.F. Nicol, A. Samuel, J. Clarke, Using results  
797 from field surveys to predict the effect of open windows on thermal comfort and  
798 energy use in buildings, *Energy Build.* 39 (2007) 823–836.  
799 doi:10.1016/j.enbuild.2007.02.003.
- 800 [18] I.A. Raja, J.F. Nicol, K.J. McCartney, M.A. Humphreys, Thermal comfort : use of  
801 controls in naturally ventilated buildings, *Energy Build.* 33 (2001) 235–244.
- 802 [19] T. Psomas, P. Heiselberg, T. Lyne, K. Duer, Automated roof window control system  
803 to address overheating on renovated houses : Summertime assessment and  
804 intercomparison, *Energy Build.* 138 (2017) 35–46. doi:10.1016/j.enbuild.2016.12.019.
- 805 [20] T. Psomas, P. Heiselberg, K. Duer, E. Bjørn, Overheating risk barriers to energy  
806 renovations of single family houses : Multicriteria analysis and assessment, *Energy*  
807 *Build.* 117 (2016) 138–148. doi:10.1016/j.enbuild.2016.02.031.
- 808 [21] S. Aggrholm, Perceived Barriers to Natural Ventilation Design of Office Buildings,  
809 1998.
- 810 [22] M. Fiorentini, G. Kokogiannakis, W. Jackson, Z. Ma, Evaluation Methodology and  
811 Implementation for Natural Ventilation Control Strategies, *Clima 2016 - RHEVA*  
812 *World Congr. Aalborg.* (2016).
- 813 [23] R. Forgiarini, N. Giraldo, R. Lamberts, A review of human thermal comfort in the built  
814 environment, *Energy Build.* 105 (2015) 178–205. doi:10.1016/j.enbuild.2015.07.047.
- 815 [24] S. Carlucci, L. Pagliano, A review of indices for the long-term evaluation of the



816 general thermal comfort conditions in buildings, *Energy Build.* 53 (2012) 194–205.  
817 doi:10.1016/j.enbuild.2012.06.015.

818 [25] S. Attia, S. Carlucci, Impact of different thermal comfort models on zero energy  
819 residential buildings in hot climate, *Energy Build.* 102 (2015) 117–128.  
820 doi:10.1016/j.enbuild.2015.05.017.

821 [26] D.H. Kang, P.H. Mo, D.H. Choi, S.Y. Song, M.S. Yeo, K.W. Kim, Effect of MRT  
822 variation on the energy consumption in a PMV-controlled office, *Build. Environ.* 45  
823 (2010) 1914–1922. doi:10.1016/j.buildenv.2010.02.020.

824 [27] S.K. Gupta, S. Atkinson, I. O’Boyle, J. Drogo, K. Kar, S. Mishra, J.T. Wen, BEES:  
825 Real-time occupant feedback and environmental learning framework for collaborative  
826 thermal management in multi-zone, multi-occupant buildings, *Energy Build.* 125  
827 (2016) 142–152. doi:10.1016/j.enbuild.2016.04.084.

828 [28] X. Fu, D. Wu, Comparison of the efficiency of building hybrid ventilation systems  
829 with different thermal comfort models, *Energy Procedia.* 78 (2015) 2820–2825.  
830 doi:10.1016/j.egypro.2015.11.640.

831 [29] P. May-Ostendorp, G.P. Henze, C.D. Corbin, B. Rajagopalan, C. Felsmann, Model-  
832 predictive control of mixed-mode buildings with rule extraction, *Build. Environ.* 46  
833 (2011) 428–437. doi:10.1016/j.buildenv.2010.08.004.

834 [30] J. Zhao, K. Poh, B.E. Ydstie, V. Loftness, Occupant-oriented mixed-mode EnergyPlus  
835 predictive control simulation, *Energy Build.* 117 (2016) 362–371.  
836 doi:10.1016/j.enbuild.2015.09.027.

837 [31] J. Hu, P. Karava, A state-space modeling approach and multi-level optimization  
838 algorithm for predictive control of multi-zone buildings with mixed-mode cooling,  
839 *Build. Environ.* 80 (2014) 259–273. doi:10.1016/j.buildenv.2014.05.003.

- 840 [32] J. Hu, P. Karava, Model predictive control strategies for buildings with mixed-mode  
841 cooling, *Build. Environ.* 71 (2014) 233–244. doi:10.1016/j.buildenv.2013.09.005.
- 842 [33] H.C. Spindler, L.K. Norford, Naturally ventilated and mixed-mode buildings d Part II :  
843 Optimal control, *Build. Environ.* 44 (2009) 750–761.  
844 doi:10.1016/j.buildenv.2008.05.018.
- 845 [34] H.C. Spindler, L.K. Norford, Naturally ventilated and mixed-mode buildings d Part I:  
846 Thermal modeling, *Build. Environ.* 44 (2009) 736–749.  
847 doi:10.1016/j.buildenv.2008.05.019.
- 848 [35] J. Chen, G. Augenbroe, X. Song, Lighted-weighted model predictive control for hybrid  
849 ventilation operation based on clusters of neural network models, *Autom. Constr.* 89  
850 (2018) 250–265. doi:10.1016/j.autcon.2018.02.014.
- 851 [36] E. Barbadilla-martín, J. Guadix, J. Manuel, S. Lissén, J. Sánchez, S. Álvarez,  
852 Assessment of thermal comfort and energy savings in a field study on adaptive  
853 comfort with application for mixed mode offices, *Energy Build.* 167 (2018) 281–289.  
854 doi:10.1016/j.enbuild.2018.02.033.
- 855 [37] R. Forgiarini, R. De Dear, E. Ghisi, Field study of mixed-mode office buildings in  
856 Southern Brazil using an adaptive thermal comfort framework, *Energy Build.* 158  
857 (2018) 1475–1486. doi:10.1016/j.enbuild.2017.11.047.
- 858 [38] G. Martín, E. Barbadilla-martín, P. Aparicio-ruiz, L. Brotas, Field study on adaptive  
859 thermal comfort in mixed mode office buildings in southwestern area of Spain Manuel  
860 Salmer o, *Build. Environ.* 123 (2017) 163–175. doi:10.1016/j.buildenv.2017.06.042.
- 861 [39] X. Deng, G. Kokogiannakis, Z. Ma, P. Cooper, Thermal comfort evaluation of a  
862 mixed-mode ventilated office building with advanced natural ventilation and  
863 underfloor air distribution systems, *Energy Procedia.* 111 (2017) 520–529.

doi:10.1016/j.egypro.2017.03.214.

[40] R. De Vecchi, C. Candido, R. De Dear, R. Lamberts, Thermal comfort in office buildings : Findings from a field study in mixed-mode and fully-air conditioning environments under humid subtropical conditions, *Build. Environ.* 123 (2017) 672–683. doi:10.1016/j.buildenv.2017.07.029.

[41] M. Lou, B. Cao, J. Damien, L. Borong, Z. Yingxin, Evaluating thermal comfort in mixed-mode buildings : A field study in a subtropical climate, *Build. Environ.* 88 (2015) 46–54. doi:10.1016/j.buildenv.2014.06.019.

[42] A.C. Boerstra, J. Van Hoof, A.M. Van Weele, A new hybrid thermal comfort guideline for the Netherlands : background and development, *Archit. Sci. Rev.* 58 (2014) 24–34. doi:10.1080/00038628.2014.971702.

[43] ASHRAE, Standard 55 - Thermal environmental conditions for human occupancy, (2017).

[44] ASHRAE, 2017 ASHRAE Handbook - Fundamentals (SI Edition), American Society of Heating, Refrigerating and Air-Conditioning Engineers, Inc., 2017.

[45] ISO/TC159/SC5, ISO 7730:2005 - Ergonomics of the thermal environment -- Analytical determination and interpretation of thermal comfort using calculation of the PMV and PPD indices and local thermal comfort criteria, (2005).

[46] B.W. Olesen, K.C. Parsons, Introduction to thermal comfort standards and to the proposed new version of EN ISO 7730, *Energy Build.* 34 (2002) 537–548. doi:10.1016/S0378-7788(02)00004-X.

[47] OASIS, oBIX, <http://www.obix.org/> (accessed January 11, 2019).

[48] T. Psomas, M. Fiorentini, G. Kokogiannakis, P. Heiselberg, Ventilative cooling

887 through automated window opening control systems to address thermal discomfort risk  
888 during the summer period: Framework, simulation and parametric analysis, Energy  
889 Build. 153 (2017). doi:10.1016/j.enbuild.2017.07.088.

890 [49] Lawrence Berkeley National Laboratories, Building Controls Virtual Test Bed  
891 (BCVTB). <https://simulationresearch.lbl.gov/bcvtb> (accessed June 25, 2019)

892